Soil Dynamics and Earthquake Engineering 141 (2021) 106467

Contents lists available at ScienceDirect

Soil Dynamics and Earthquake Engineering

journal homepage: http://www.elsevier.com/locate/soildyn

Generation of fully non-stationary random processes consistent with target seismic accelerograms

G. Muscolino, F. Genovese *, G. Biondi, E. Cascone

Department of Engineering, University of Messina, 98166, Messina, Italy

ARTICLE INFO

Keywords:
Artificial accelerograms
Fully non-stationary stochastic process
Evolutionary power spectral density function
Real ground motion records
Simulation

ABSTRACT

In this paper, a method for generating samples of a *fully non-stationary* zero-mean Gaussian process, having a target acceleration time-history as one of its own samples, is presented. The proposed method requires the following steps: i) divide the time axis of the target accelerogram in contiguous time intervals in which a *uniformly modulated* process is introduced as the product of a deterministic *modulating function* per a stationary zero-mean Gaussian sub-process, whose *power spectral density* (*PSD*) function is filtered by two Butterworth filters; ii) estimate, in the various time intervals, the parameters of *modulating functions* by least-square fitting the expected energy of the proposed model to the energy of the target accelerogram; iii) estimate the parameters of the *PSD* function of the stationary sub-process, once the occurrences of maxima and of *zero-level up-crossings* of the target accelerogram, in the various intervals, are counted; iv) obtain the evolutionary spectral representation of the *fully non-stationary* process by adding the various contribution evaluated in the various intervals.

1. Introduction

Strong motion earthquakes represent critical actions for most *Structural and Geotechnical* (*S&G*) *systems* located in seismically active regions. The analysis of recorded accelerograms after earthquakes evidences that different earthquakes produce ground motions with different characteristics in terms of intensity, duration, destructiveness, dominant periods and frequency content. It follows that, in order to guarantee a good performance of *S&G systems* in seismic areas, it needs to adequately characterise the ground motion acceleration [1].

The worldwide increasing availability of recorded accelerograms makes the use of these time-histories an attractive option to properly define the motions to be used as input in dynamic analysis of both *S&G systems*. According to most seismic codes, the selection of proper sets of input motions for these kinds of analyses is generally carried out defining a target motion through a design elastic pseudo-acceleration response spectrum [2].

The results of the selection procedure is influenced by multiple sources of uncertainties related to the definition of the seismic hazard at the site of interest, to the criteria adopted to check the compatibility of the selected records with the frequency and energy content of a target motion expected at the site of interest [3] and to the combined effects of frequency coupling and soil non-linear behaviour which significantly affect the characteristics of the ground motion expected at the site.

Different procedures for the selection of sets of recorded accelerograms have been proposed in the literature [e.g. 4–6]. Several recent studies have clearly pointed out the crucial role of the geotechnical properties of soils at the site of interest, relevant in seismic perspective, and the need of defining proper target energy and frequency contents instead of, or together with, target elastic response spectra. As an example, in Ref. [7,8], with reference to 1D site response analyses, it is demonstrated that soil heterogeneity in terms of shear wave velocity profile and soil non-linear behaviour under cyclic loading significantly affect the interval of vibration periods relevant for the accelerogram selection and the characteristics of the selected input motions. Furthermore, Lanzo et al. [9] and Cascone et al. [10] pointed out the need of using target values of Arias intensity for a proper selection of input motions to be used in 2D non-linear analyses of the seismic response of earth-dams.

However, depending on the characteristics of the target ground motion and on the adopted compatibility criterion, it may be impossible to select an adequate number of compatible accelerograms (i) actually reflecting the influence of the expected focal mechanism, (ii) reliably compatible with the magnitude and site-to-source distance that dominate the seismic hazard at the site of interest and, finally, (iii) without applying large acceleration scale factors which distort the actual

* Corresponding author.
E-mail addresses: gmuscolino@unime.it (G. Muscolino), fedgenovese@unime.it (F. Genovese), gbiondi@unime.it (G. Biondi), ecascone@unime.it (E. Cascone).

https://doi.org/10.1016/j.soildyn.2020.106467
Received 15 May 2020; Received in revised form 31 July 2020; Accepted 7 September 2020
Available online 26 December 2020

characteristics of the un-scaled records leading to unrealistic input motions. In these situations, the use of artificial accelerograms represents a suitable alternative to realistically define the expected ground motion.

The generation of *artificial accelerograms* was first based upon a stationary stochastic zero-mean Gaussian process assumption. In particular, *stationary white-noise* ground-motion models were proposed by Housner [11] and Bycroft [12]. Successively, to account for the frequency content of earthquake ground motion, Gaussian filtered white noise with Kanai-Tajimi [13,14] or Clough-Penzien [15] spectra are frequently used in analytical random vibration analyses. Housner and Jennings [16] developed a method for generating filtered stationary Gaussian random processes with *power spectral density* (*PSD*) functions derived from the average of the undamped velocity spectra of recorded ground accelerations. These stationary models account for the site properties as well as for the dominant frequency in ground motion. However, they fail since are not able to reliably reproduce the changes in amplitude and frequency content, which are observed in actual seismic records. Faravelli [17] formulated a stationary ground-motion model with mu1timodal spectral density to reproduce frequency variation.

Moreover, it has been recognised that artificial accelerograms generated by applying stationary models have an excessive number of cycles and consequently they possess unreasonably much higher energy content with respect to real ones [3,18].

It is well known that earthquake ground motions are non-stationary in both time and frequency domains. Temporal non-stationarity refers to the variation in the intensity of the ground motion in time, whereas the spectral non-stationarity refers to the time variation of the frequency content [19]. To capture the variation in the intensity of accelerograms, non-stationary processes have been introduced as the product of the stationary zero-mean Gaussian random process by a suitable deterministic time-dependent function, the so-called *modulating function* [see 20–27]. Due to their non-stationarity in time, these are called separable non-stationary stochastic processes or more commonly: *quasi-stationary* (or *uniformly modulated non-stationary*) random processes.

Opposite to temporal non-stationarity, spectral non-stationarity is not so easy to model. For both temporal and spectral non-stationarities, seismological as well as geotechnical aspects are extremely relevant since the distribution of the ground motion intensity over the time (temporal non-stationarity) as well as the energy distribution in the frequency domain (spectral non-stationarity) are strictly related to the characteristics of the source mechanism but are also significantly influenced by the seismic waves travel path and, finally, by the complex non-linear phenomena overall denoted as site effects.

The spectral non-stationarity is prevalently due to different arrival times of the body (primary, secondary) and surface waves that propagate at different velocities through the earth crust vary significantly in frequency content and reach the ground surface at different times.

Moreover, it has been shown that the non-stationarity in frequency content can have significant effects on the response of both linear and non-linear structural [28–31] and geotechnical [32–36] systems.

Non-linear *S&G systems* tend to have resonant frequencies which decay with time as the system responds to seismic acceleration, as a consequence of non-linear effects. This trend may coincide with the variation in time of the predominant frequency of the ground motion. The stochastic processes involving both the intensity and the spectral variation in time are referred in the literature as *fully non-stationary* (or *non-separable*) stochastic processes.

Several approaches have been adopted in the literature to capture the variation in both amplitude and frequency of recorded accelerograms. In particular, by solving probabilistic energy spectra equations, Spanos [37,38] introduced evolutionary non-separable power spectra as the product of a deterministic time-frequency dependent function by the *PSD* function of stationary zero-mean Gaussian stochastic processes. Alternative very widespread *fully non-stationary* stochastic process models based on filtered processes have also been proposed. These models, whose parameters can be identified by matching with the characteristics of the target accelerogram, can be subdivided in two categories: a) stochastic processes obtained by passing a white noise through a filter with time dependent coefficients [19,28,30,39,40]; b) processes obtained by passing a train of Poisson pulses through a linear filter [41–44].

A very useful approach to generate fully non-stationary zero-mean Gaussian stochastic processes is the one based on the evolutionary spectral representation, that requires the introduction of the *Evolutionary Power Spectral Density* (*EPSD*) function [45,46]. Three main models have been proposed in the literature to evaluate *EPSD* functions whose parameters are identified from recorded accelerograms. The first was the Saragoni and Hart model [47] in which the time axis is subdivided in three contiguous segments, each with different modulating and *PSD* functions. The *modulating function* is used to control the process intensity level, while the counting of *zero-level crossings* and *peaks* are used to characterise the *PSD* functions in the three time intervals. The second model was proposed by Der Kiureghian and Crempien [48] in which the strength function of the process is changed at discrete points along the frequency axis. The resulting process is given by the superposition of independent processes with constant *PSD* function, and unitary variance, over their respective bands. This model, in a sense can be considered as the complement of the Saragoni and Hart [47] model. However, one shortcoming of this model, in the identification of its parameters, is the need to perform, in each frequency segment, the inverse Fourier transform of the Fourier transform of the accelerogram. In the third model, proposed by Conte and Peng [49], the resulting process is evaluated as the sum of a finite number of zero-mean, independent, uniformly modulated zero-mean Gaussian sub-processes, the so-called *sigma-oscillatory processes.* Each uniformly modulated process consists of the product of a real deterministic time *modulating function* and a stationary Gaussian sub-process, having unimodal *PSD* function with unitary variance. The parameters of the resulting analytical *EPSD* function are estimated in the least-square sense by using the short-time Thomson's multiple-window method. The main shortcoming of this very interesting model is the complexity of the identification procedure.

Other strategies to analyse the evolutionary frequency content of fully non-stationary stochastic processes are based on: a) the short-time Fourier transform [50,51]; b) the wavelet transform [52–54]; c) the Hilbert-Huang transform [55,56].

In this paper a method for generating samples of a *fully non-stationary* zero-mean Gaussian process, having an actual acceleration record as one of its own samples, is presented.

To this purpose, the time duration of the accelerogram is divided in some contiguous time intervals in which zero-mean Gaussian *uniformly modulated* stochastic processes are adopted. Each *uniformly modulated* random process consists of the product of a positive deterministic *modulating function*, and a stationary zero-mean Gaussian sub-process, whose *PSD* function is filtered by one high pass and one low pass Butterworth filters. It follows that the Priestley's evolutionary *EPSD* function is evaluated by adding the contributions of all zero-mean Gaussian *uniformly modulated* stochastic processes. In the considered time intervals a polynomial or an exponential decaying form of the *modulating function* is assumed. The order of the polynomials and their coefficients are estimated by least-square fitting, in each time interval, the expected energy of the proposed model of the fully non-stationary process to the energy of the target accelerogram. Then, in each interval the parameters of the *PSD* function of the stationary sub-process are estimated once the occurrences of maxima and the occurrences of crossings of the time-axis with positive slope of the target accelerograms are counted. Finally, the parameters of Butterworth filter are opportunely chosen.

The analytical form of the *modulating functions* in the various intervals have been chosen with the purpose to obtain functions that permit to evaluate closed form solutions of the *EPSD* function of the seismic response of *S&G systems* in seismic areas [see 57]. This goal cannot be achieved by adopting the *modulating function* of the Saragoni

Table 1
Main characteristics of the selected accelerograms.

$n°$	Earthquake Name	Station and Event Date	M_w	R_{JB} [km]	a_{max} [m/s^2]	$v_{s,30}$ [m/s]	T_D [s]	*SMD* [s]	I_0 [m^2/s^3]	I_A [m/s]	N_0^+	P_0
1	Kern County	Taft Lincoln School – 21 21/07/1952	7.36	38.42	1.55	385.43	54.34	30.28	3.44	0.55	163	289
2	Kern County	Taft Lincoln School – 111 21/07/1952	7.36	38.42	1.76	385.43	54.36	28.77	3.73	0.59	167	295
3	Kobe, Japan	Kakogawa – 0 16/01/1995	6.90	22.5	2.35	312.00	40.95	13.15	6.43	1.03	154	259
4	Kobe, Japan	Kakogawa – 90 16/01/1995	6.90	22.5	3.18	312.00	40.95	12.85	10.53	1.68	134	264
5	Friuli, Italy – 02	Forgaria Cornino – 0 15/09/1976	5.91	14.65	2.56	412.37	21.98	4.49	1.82	0.29	116	196
6	Friuli, Italy – 02	Forgaria Cornino – 270 15/09/1976	5.91	14.65	2.07	412.37	21.98	4.57	2.33	0.37	99	204
7	Kocaeli, Turkey	Yarimca – 60 17/08/1999	7.51	1.38	2.22	297.00	28.99	15.09	8.30	1.32	60	112
8	Kocaeli, Turkey	Yarimca – 150 17/08/1999	7.51	1.38	3.15	297.00	28.99	15.07	8.26	1.32	71	260

Table 2
Parameters of the modulating function selected for the accelerograms listed in Table 1.

$n°$	t_1 [s]	t_2 [s]	k_1%	k_2%	p	D_p [m/s^2]	$\lvert\ddot{U}_g(T_D)\rvert$ [m/s^2]
1	3.13	40.58	1	98	7	0.167	0.00275
2	3.45	25.82	3	91	7	0.171	0.00758
3	2.55	14.22	1	91	10	0.247	0.00210
4	2.63	26.47	1	99	9	0.308	0.00084
5	2.51	6.84	2	90	5	0.192	0.00134
6	3.33	7.55	4	94	9	0.191	0.00114
7	2.55	14.10	1	91	8	0.285	0.02539
8	3.31	14.55	3	91	10	0.310	0.01282

and Hart [47] model.

The paper is organised as follows. In Section 2, a brief summary of the fundamentals of the evolutionary spectral representation of *fully non-stationary* zero-mean Gaussian stochastic processes is presented. Section 3 outlines the proposed evolutionary model for the *fully non-stationary* stochastic process. In Section 4 a method for the estimation of both *modulating function* and *PSD* function of stationary sub-processes parameters, from target accelerograms, is described. Finally, in Section 5, eight accelerograms relative to four seismic events are analysed to show the accuracy and computational efficiency of the proposed method.

2. Evolutionary spectral representation of fully non-stationary zero-mean Gaussian stochastic processes

A zero-mean Gaussian fully non-stationary random process $F_0(t)$, is usually represented by the evolutionary spectral Priestley's model [45, 46]. Moreover, in the stochastic analysis the one-sided *Power Spectral Density* (*PSD*) function is generally used to characterise the input process. It has been demonstrated that, since the one-sided *PSD* function is not symmetric [58–60], the corresponding autocorrelation function is a complex function having real part coincident with the autocorrelation function corresponding to the two-sided *PSD* [59]. This implies that, from a mathematical point of view, the zero-mean Gaussian fully non-stationary random process is a complex process too. It can be defined by means of the following *Fourier-Stieltjes integral*:

$$F_0(t) = \int_0^{\infty} \exp(\mathrm{i}\omega t)\, a(\omega, t)\, \mathrm{d}N(\omega) \tag{1}$$

where $\mathrm{i} = \sqrt{-1}$ is the imaginary unit; $a(\omega, t)$ is a slowly varying complex deterministic time-frequency *modulating function*, which has to satisfy the conditions: $a(\omega,t) \equiv a^*(-\omega,t), \mathrm{Re}\{a(\omega,t)\} \geq 0$; $N(\omega)$ is a zero-mean process with orthogonal increments satisfying the condition:

$$\mathrm{E}\langle \mathrm{d}N(\omega_1)\, \mathrm{d}N^*(\omega_2)\rangle = \frac{1}{2}\delta(\omega_1 - \omega_2)\, G_0(\omega_1)\mathrm{d}\omega_1\, \mathrm{d}\omega_2 \tag{2}$$

where the operator $\mathrm{E}\langle \bullet \rangle$ denotes the stochastic average; the asterisk * indicates complex conjugate quantities; $\delta(\bullet)$ is the Dirac delta, and $G_0(\omega)$ is the one-sided *PSD* function of the "embedded" stationary counterpart process [61], which is a real function for $\omega \geq 0$, while $G_0(\omega) = 0$ for $\omega < 0$.

Notice that, because of the PSD function has been assumed one-sided, the zero-mean Gaussian non-stationary random process $F_0(t)$ is a complex one [58–60] that can be defined, in the time domain, by the knowledge of its complex autocorrelation function:

$$R_{F_0F_0}(t_1, t_2) \equiv \mathrm{E}\langle F_0(t_1)\, F_0(t_2)\rangle = \\ = \int_0^{\infty} \exp[\mathrm{i}\omega(t_1 - t_2)]G_{F_0F_0}(\omega, t_1, t_2)\mathrm{d}\omega \tag{3}$$

where:

$$G_{F_0F_0}(\omega, t_1, t_2) = a(\omega, t_1)\, a^*(\omega, t_2)G_0(\omega) \tag{4}$$

Table 3
Polynomial coefficients [m/s^{i+2}] in the first two time intervals of the modulating functions of the selected accelerograms.

$n°$	$0 \leq t < t_1$		$t_1 \leq t < t_2$									
	α_1	α_2	α_1	α_2	α_3	α_4	α_5	α_6	α_7	α_8	α_9	α_{10}
1	$8.6{\cdot}10^{-3}$	0.020	0.226	−0.054	$5.6{\cdot}10^{-3}$	$-3.38{\cdot}10^{-4}$	$1.1{\cdot}10^{-5}$	−1.97	$1.4{\cdot}10^{-9}$	–	–	–
2	$3.7{\cdot}10^{-4}$	0.028	0.513	−0.247	0.050	−0.005	$3.1{\cdot}10^{-4}$	$-9.6{\cdot}10^{-6}$	$1.1{\cdot}10^{-7}$	–	–	–
3	$1.5{\cdot}10^{-3}$	0.051	1.679	−3.106	2.529	−1.101	0.284	−0.045	$4.5{\cdot}10^{-3}$	$-2.7{\cdot}10^{-4}$	$8.9{\cdot}10^{-6}$	$-1.2{\cdot}10^{-7}$
4	$1.8{\cdot}10^{-4}$	0.056	1.246	−0.857	0.290	−0.054	$5.8{\cdot}10^{-3}$	$-3.8{\cdot}10^{-4}$	$1.4{\cdot}10^{-5}$	$-3.0{\cdot}10^{-7}$	$2.7{\cdot}10^{-9}$	–
5	0.071	$5.0{\cdot}10^{-4}$	0.309	1.251	−1.207	0.358	−0.034	–	–	–	–	–
6	0.067	$4.6{\cdot}10^{-3}$	6.505	−22.109	34.227	−27.535	12.101	−2.842	0.296	$2.6{\cdot}10^{-4}$	$-1.6{\cdot}10^{-3}$	–
7	0.130	$6.8{\cdot}10^{-5}$	1.680	−1.725	0.916	−0.283	0.051	−0.005	$2.9{\cdot}10^{-4}$	$-6.6{\cdot}10^{-6}$	–	–
8	0.125	$1.3{\cdot}10^{-4}$	5.799	−11.743	10.432	−5.114	1.522	−0.286	0.034	$2.5{\cdot}10^{-3}$	$1.0{\cdot}10^{-4}$	$1.8{\cdot}10^{-6}$

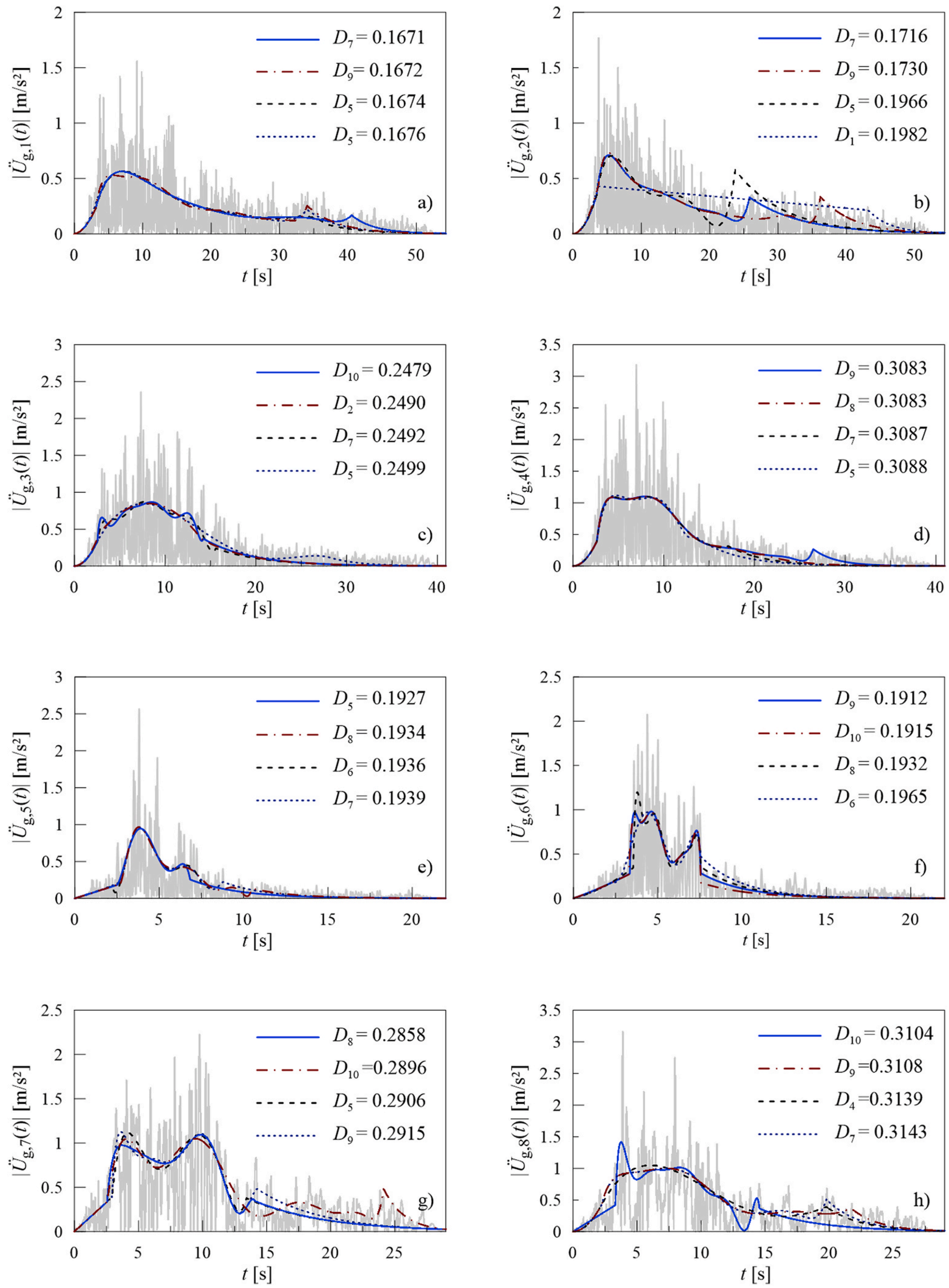

Fig. 1. Absolute value of the analysed accelerograms and selected *modulating functions* $a(t)$, having the smaller *rms* difference D_p: a) Taft Lincoln School-21; b) Taft Lincoln School-111; c) Kakogawa-0; d) Kakogawa-90; e) Forgaria Cornino-0; f) Forgaria Cornino-270; g) Yarimca-60; h) Yarimca-150.

The complex process $F_0(t)$, which generates the complex autocorrelation function (3) has been called *pre-envelope process* by Di Paola [58]. In the Priestley evolutionary process model, the function

$$G_{F_0F_0}(\omega,t) = |a(\omega,t)|^2 G_0(\omega) \tag{5}$$

is called one-sided *evolutionary power spectral density* (*EPSD*) function of the non-stationary process $F_0(t)$. This process is called *fully non-stationary* random process, since both time and frequency content change. If the *modulating function* $a(\omega,t) \equiv a(t)$ is a positive time dependent real function, the non-stationary process is called *uniformly modulated* (or *quasi-stationary*) random process. In the latter case the *EPSD* function assumes the expression: $G_{F_0F_0}(\omega,t) = a(t)^2 G_0(\omega)$.

The samples of real and imaginary part of the fully non-stationary complex process $F_0(t)$, introduced in Eq. (1), can be generated, according to the procedure described in Ref. [62], by applying the following relationships [57]:

$$\begin{aligned} \overline{F}_0^{(i)}(t) \equiv \mathrm{Re}\{F_0^{(i)}(t)\} &= \sum_{k=1}^{m_c} \sqrt{2G_{F_0F_0}(\omega_k,t)\Delta\omega}\,\sin(\omega_k\, t + \theta_k^{(i)}); \\ \mathrm{Im}\{F_0^{(i)}(t)\} &= \sum_{k=1}^{m_c} \sqrt{2G_{F_0F_0}(\omega_k,t)\Delta\omega}\,\cos(\omega_k\, t + \theta_k^{(i)})\,. \end{aligned} \tag{6}$$

In this equation $F_0^{(i)}(t)$ is the i-th sample of the process $F_0(t)$; $\Delta\omega$ is the frequency step; m_c is an integer number, chosen in such a way that the relationship $m_c = \omega_c/\Delta\omega$ is satisfied, with ω_c the upper cut-off circular frequency; $\omega_k = k\ \Delta\omega$ $(k = 1, 2, \ldots, m_c)$; $\theta_k^{(i)}$ are random phase

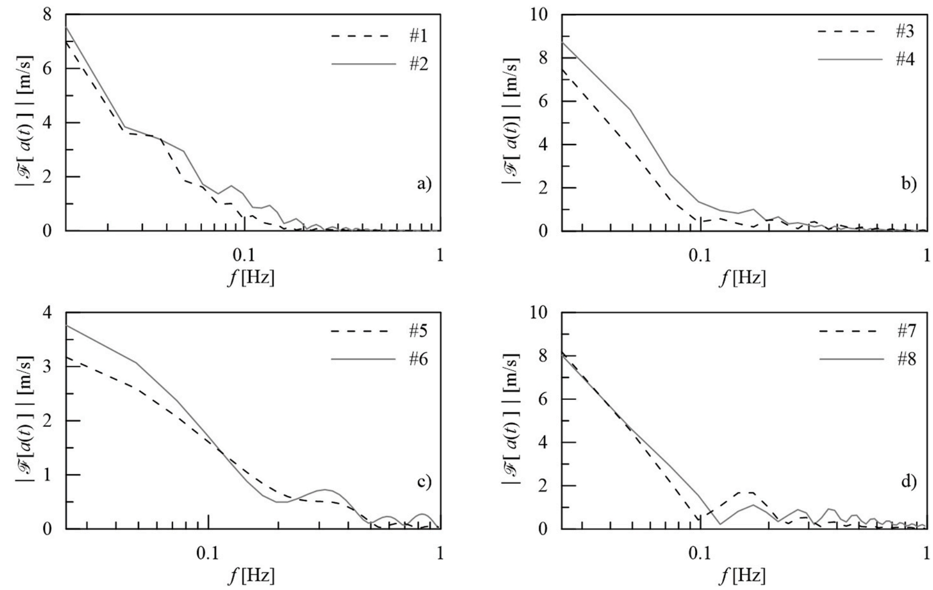

Fig. 2. Moduli of Fourier transforms of the eight modulating functions evaluated by applying the proposed procedure: a) Taft Lincoln School; b) Kakogawa; c) Forgaria Cornino; d) Yarimca.

Table 4
Main parameters of the one-sided *PSD* functions in the three time intervals analysed for each of the selected accelorograms.

$n°$	$0 \le t < t_1$						$t_1 \le t < t_2$						$t_2 \le t \le T_D$					
	$N_{0,1}^{+}$	P_1	ΔT_1 [s]	Ω_1 [rad/s]	ρ_1 [rad/s]	β_1	$N_{0,2}^{+}$	P_2	ΔT_2 [s]	Ω_2 [rad/s]	ρ_2 [rad/s]	β_2	$N_{0,3}^{+}$	P_3	ΔT_3 [s]	Ω_3 [rad/s]	ρ_3 [rad/s]	β_3
1	12	23	3.1	24.1	12.6	7.1	128	204	37.4	21.4	10.1	5.6	23	65	14.7	10.5	6.3	3.6
2	13	30	3.7	21.6	12.2	6.9	79	127	22.3	22.5	10.6	6.0	75	142	28.5	16.5	8.6	4.8
3	18	24	2.5	44.5	18.2	10.2	52	77	11.6	28.0	12.5	7.0	84	166	26.7	19.7	10.5	5.9
4	14	29	2.6	33.5	18.2	10.3	89	151	23.8	23.4	11.5	6.4	31	91	14.4	13.4	8.2	4.7
5	21	30	2.5	52.5	22.8	12.8	26	33	4.3	37.8	14.8	8.2	69	138	15.1	28.6	15.3	8.6
6	26	40	3.3	49.0	22.5	12.6	20	26	4.2	29.8	11.9	6.6	53	140	14.4	23.0	13.7	7.8
7	15	39	2.5	36.9	21.9	12.4	21	82	11.5	11.4	7.5	4.2	24	99	14.8	10.1	6.7	3.8
8	23	55	3.3	43.7	25.1	14.2	18	103	11.2	10.0	7.0	4.0	30	110	14.4	13.0	8.4	4.8

angles uniformly distributed over the interval $[0-2\pi)$. Notice that the random phase angle, $\theta_k^{(i)}$, must be the same in both Eq. (6), to simultaneously obtain the real and imaginary part of the i-th sample of the complex process $F_0(t)$ [57].

3. Evolutionary model for earthquake-induced ground acceleration

In this paper, the *fully non-stationary* model of earthquake ground acceleration is defined as the sum of zero-mean Gaussian *uniformly modulated* stochastic processes. Each *uniformly modulated* random process consists of the product of a positive deterministic *modulating function*, $a(t)$, and a stationary zero-mean Gaussian filtered sub-process, $X_k(t)$. Thus, according to the philosophy of Saragoni and Hart [47] model, the *fully non-stationary* stochastic process $F_0(t)$, of time duration T_D, is here obtained by dividing the time interval $0 \div T_D$ in n contiguous time intervals of amplitude $\Delta T_k = t_k - t_{k-1} (k = 1, 2\cdots, n)$ and requiring that in each time interval the sub-process $X_k(t)$, possesses a unimodal *PSD* function, that is:

$$F_0(t) = \sum_{k=1}^{n} F_{0,k}(t) = \sum_{k=1}^{n} a(t)\, X_k(t)\ \ \mathbb{W}(t_{k-1}, t_k) \tag{7}$$

where $\mathbb{W}(t_{k-1}, t_k) = \mathbb{U}(t - t_k) - \mathbb{U}(t - t_{k-1})$ is the window function, with $\mathbb{U}(t)$ the unit step function. Moreover, in the time interval $[t_{k-1}, t_k)$, the sub-process $X_k(t)$ is here characterised by the following one-sided *PSD* function:

$$G_{X_k}(\omega) = \beta_k \left(\frac{\omega^2}{\omega^2 + \omega_{H,k}^2}\right)\left(\frac{\omega_{L,k}^4}{\omega^4 + \omega_{L,k}^4}\right) G_k^{(CP)}(\omega); \quad k = 1, \dots, n \tag{8}$$

where $\omega_{L,k}$ and $\omega_{H,k}$ are the k-th frequency control of the second order low pass and first order high pass Butterworth filters, respectively, $G_k^{(CP)}(\omega)$ is a unimodal one-sided *PSD* function, having unit area, which can be viewed as the linear combination of the displacement and velocity responses of a second-order oscillator subjected to two statistically independent Gaussian white noise processes [49]:

$$G_k^{(CP)}(\omega) = \frac{\rho_k}{\pi}\left(\frac{1}{\rho_k^2 + (\omega + \Omega_k)^2} + \frac{1}{\rho_k^2 + (\omega - \Omega_k)^2}\right); \quad k = 1, \dots, n \tag{9}$$

In this equation ρ_k and Ω_k are two free parameters. The first one is a circular frequency bandwidth, the second one is close enough to the predominant circular frequency of the k-th filtered stationary process [49]. Finally, in Eq. (8) the coefficient β_k is evaluated in such a way that the sub-process $X_k(t)$ possesses unit variance $\mathrm{E}\langle X_k^2(t)\rangle \equiv \sigma_{X_k}^2 = 1$. It is given in closed form solution as follows:

$$\beta_k = \frac{2\, \overline{a}_k \overline{b}_k \left(\omega_{H,k}^4 + \omega_{L,k}^4\right)}{\omega_{L,k}^3 \left(\overline{c}_k + \overline{d}_k + \overline{e}_k\right)} \tag{10}$$

where:

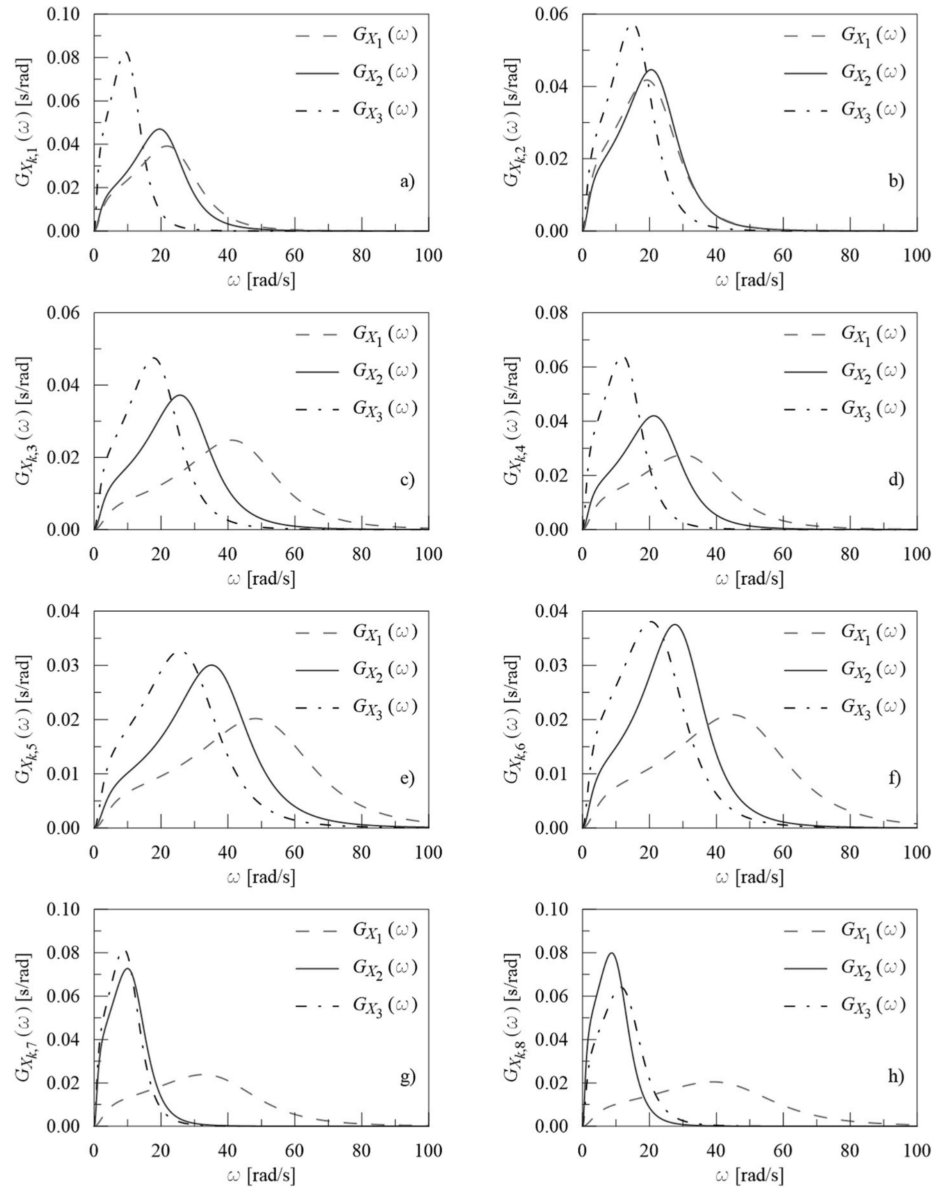

Fig. 3. One-sided *PSD* functions in the three contiguous time intervals, of the selected accelerograms: a) Taft Lincoln School-21; b) Taft Lincoln School-111; c) Kakogawa-0; d) Kakogawa-90; e) Forgaria Cornino-0; f) Forgaria Cornino-270; g) Yarimca-60; h) Yarimca-150.

$$
\begin{aligned}
\overline{a}_k &= \left(\rho_k^2+\Omega_k^2\right)^4+2\left(\rho_k^4-6\rho_k^2\Omega_k^2+\Omega_k^4\right)\omega_{L,k}^4+\omega_{L,k}^8;\\
\overline{b}_k &= \rho_k^4+2\rho_k^2\left(\Omega_k^2-\omega_{H,k}^2\right)+\left(\Omega_k^2+\omega_{H,k}^2\right)^2;\\
\overline{c}_k &= \left[\left(\rho_k^2+\Omega_k^2\right)^2\left(\rho_k^4-6\rho_k^2\Omega_k^2+\Omega_k^4+\omega_{L,k}^4\right)-\omega_{H,k}^2\left(\rho_k^2-\Omega_k^2\right)\left(\left(\rho_k^2+\Omega_k^2\right)^2+\omega_{L,k}^4\right)\right]\times 2\omega_{L,k}\left(\omega_{H,k}^4+\omega_{L,k}^4\right);\\
\overline{d}_k &= -2\,\overline{a}_k\,\rho_k\,\omega_{H,k}\,\omega_{L,k}\left(\rho_k^2+\Omega_k^2-\omega_{H,k}^2\right);\\
\overline{e}_k &= \sqrt{2}\,\overline{b}_k\,\rho_k\left\{\omega_{L,k}^2\left(\omega_{H,k}^2-\omega_{L,k}^2\right)\left(\omega_{L,k}^4+\rho_k^4-2\rho_k^2\Omega_k^2-3\Omega_k^4\right)+\left(\omega_{H,k}^2+\omega_{L,k}^2\right)\left[\rho_k^6+\Omega_k^6+3\Omega_k^2\rho_k^2\left(\rho_k^2+\Omega_k^2\right)+\omega_{L,k}^4\left(\rho_k^2-3\Omega_k^2\right)\right]\right\}.
\end{aligned}
\tag{11}
$$

Scaling the *PSD* function (8) to have unit variance allows separating, in each time interval, the time variation in amplitude from the frequency content of the various segments of the stochastic process $F_0(t)$.

It has to be emphasised that the unimodal *PSD* function $G_k^{(CP)}(\omega)$ of the Conte and Peng [49] model behaves like ω^{-2} for ω tending to infinite and this shows that $\omega^i\, G_k^{(CP)}(\omega)$ for $i \geq 1$ is not integrable. So the spectral

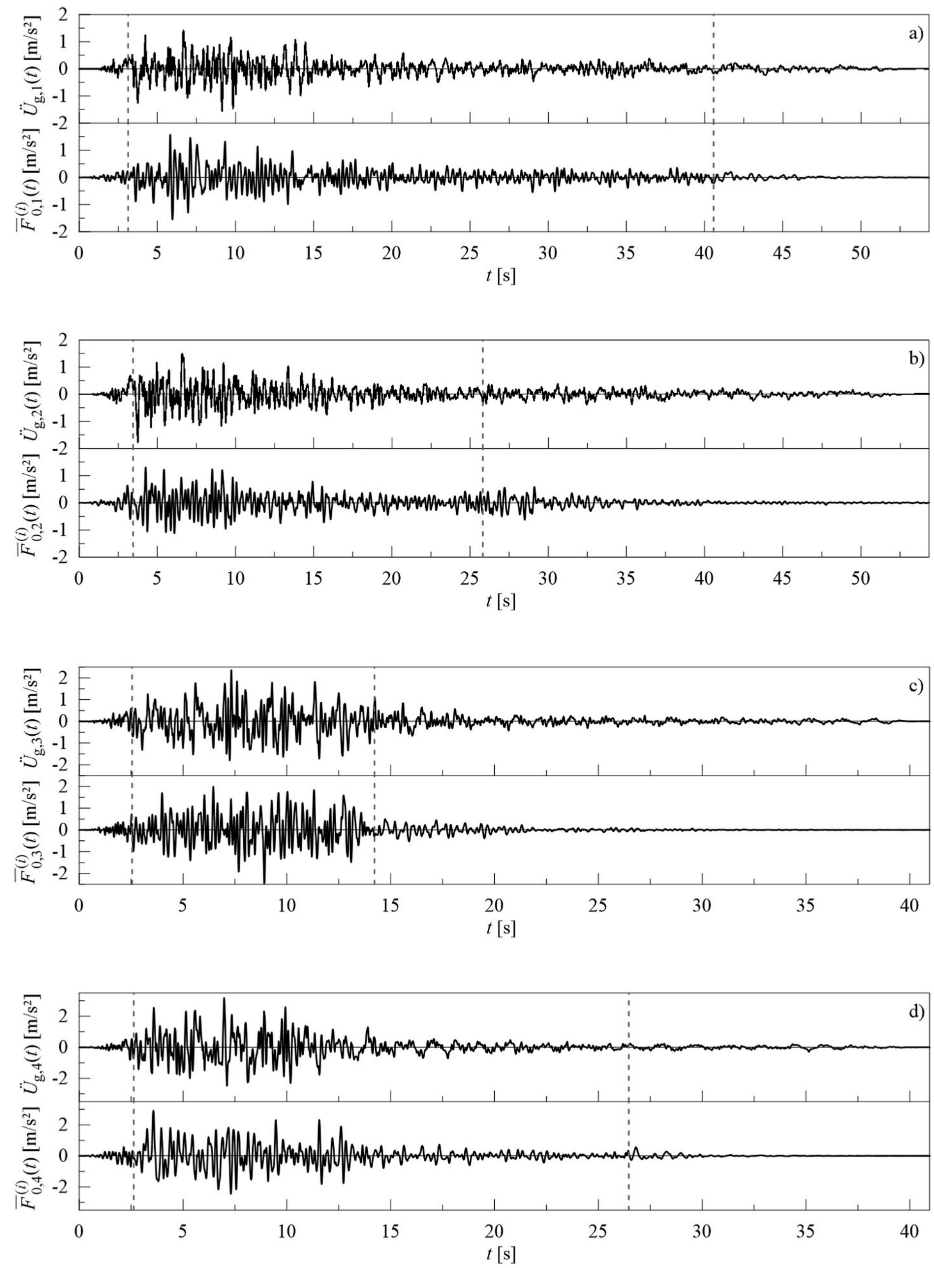

Fig. 4. Comparison between the selected horizontal and the corresponding i-th generated samples $\overline{F}^{(i)}_{0,\ell}$. The vertical dashed lines delimit the three time intervals: a) Taft Lincoln School-21; b) Taft Lincoln School-111; c) Kakogawa-0; d) Kakogawa-90; e) Forgaria Cornino-0; f) Forgaria Cornino-270; g) Yarimca-60; h) Yarimca-150.

moments of the function $G_k^{(CP)}(\omega)$ of order greater than zero are divergent quantities. Moreover, the *PSD* function $G_k^{(CP)}(\omega)$ presents frequency distortion at very low frequencies. To avoid these two drawbacks of $G_k^{(CP)}(\omega)$ function, in this paper, respectively, second order low pass Butterworth filters, with k-th frequency control $\omega_{L,k}$, and first order high pass Butterworth filters, with k-th frequency control $\omega_{H,k}$, have been introduced in Eq. (8), to characterise the one-sided *PSD* function of the k-th sub-process $X_k(t)$.

Finally, the one-sided *EPSD* function for the proposed model results:

$$G_{F_0F_0}(\omega,t) = \sum_{k=1}^{n} a^2(t)\mathbb{W}(t_{k-1},t_k)G_{X_k}(\omega) \equiv \sum_{k=1}^{n} G_{X_k}(\omega,t) \tag{12}$$

Furthermore, since each sub-process possesses unit variance, the time-dependent variance of the *fully non-stationary* process $F_0(t)$ is given as:

$$\sigma^2_{F_0}(t) \equiv \mathrm{E}\langle F_0^2(t)\rangle = \int_0^\infty G_{F_0F_0}(\omega,t)\mathrm{d}\omega = \sum_{k=1}^{n} a^2(t)\,\mathbb{W}(t_{k-1},t_k) \tag{13}$$

Note that, the *EPSD* function (12) describes simultaneously the time-varying intensity and the time-varying frequency content. It follows that $F_0(t)$ is *fully-non stationary*, although its component processes are individually *uniformly modulated*. Therefore, each *uniformly modulated* sub-process $X_k(t)$, characterised by a *PSD* function in the frequency domain and a *modulating function* in the time domain, captures, in its time interval, a group of seismic waves possessing a specific time-frequency distribution of earthquake-induced ground motion acceleration.

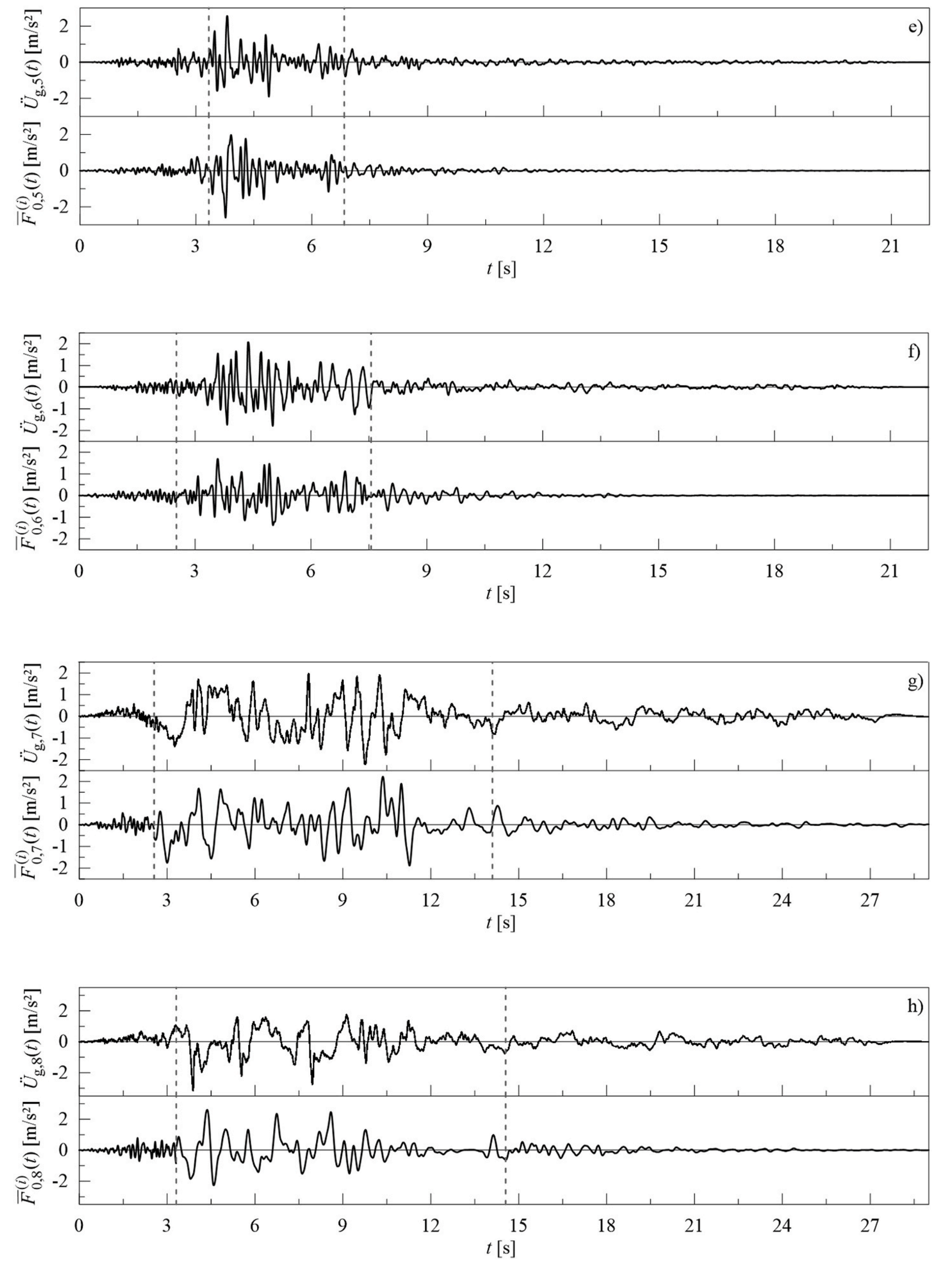

Fig. 4. (*continued*).

4. Parameters estimation from target accelerograms

In the previous section a *fully non-stationary* model of earthquake ground acceleration has been described. The purpose of this section is to define a stochastic process $F_0(t)$ such that the target accelerogram, $\ddot{U}_g(t)$, may be considered as one of its samples. To do this the *modulating function* and the frequency content of the process $F_0(t)$ can be estimated separately.

4.1. Estimation of modulating function

Let us consider a target accelerogram $\ddot{U}_g(t)$ of time duration T_D. To evaluate the *modulating function*, $a(t)$, the time interval $0 \div T_D$ is subdivided in n_a contiguous time intervals of amplitude $\Delta T_j = t_j - t_{j-1}$ $(j = 1, 2, \cdots, m, \cdots n_a)$. The cumulative energy function of the target accelerogram is evaluated as:

$$E_{\ddot{U}_g}(t) = \int_0^t \ddot{U}_g^2(\tau)\,\mathrm{d}\tau = \sum_{j=1}^{m \le n_a} \int_{t_{j-1}}^{t_j} \ddot{U}_g^2(\tau)\mathrm{d}\tau; \quad 0 \le t \le T_D \tag{14}$$

Moreover, $E_{\ddot{U}_g}(T_D) \equiv I_0$ is the so-called *total intensity* of the ground motion acceleration [63]. Remembering that in each time interval the sub-processes $X_j(t)$, in Eq. (7), possess unitary variance as well as the definition (13) of the time-dependent variance of the *fully non-stationary* process, the *cumulative expected energy* function of the stochastic process $F_0(t)$ can be evaluated as [47]:

$$\mathrm{E}\langle E_{F_0}(t)\rangle = \int_0^t \mathrm{E}\langle F_0^2(\tau)\rangle\,\mathrm{d}\tau \equiv \int_0^t \sigma_{F_0}^2(\tau)\,\mathrm{d}\tau = \sum_{j=1}^{m \le n_a} \int_{t_{j-1}}^{t_j} a^2(\tau)\,\mathrm{d}\tau \tag{15}$$

To estimate $a(t)$, in the j-th time interval $[t_{j-1}, t_j)$, the *function* $\psi_j(t)$ is introduced:

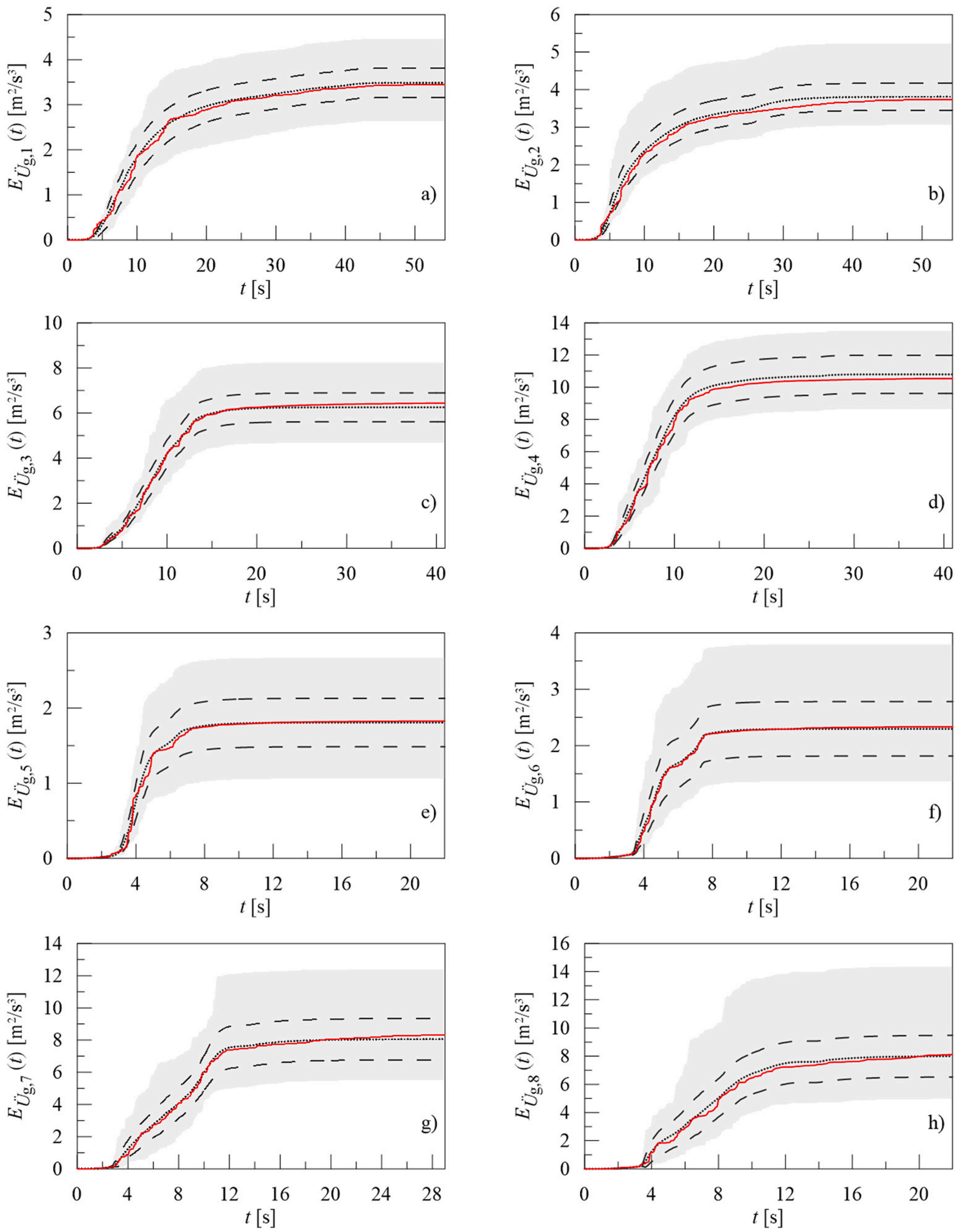

Fig. 5. Comparison among the energy functions of the selected accelerograms with statistics of the artificial ones: a) Taft Lincoln School-21; b) Taft Lincoln School-111; c) Kakogawa-0; d) Kakogawa-90; e) Forgaria Cornino-0; f) Forgaria Cornino-270; g) Yarimca-60; h) Yarimca-150. Target accelerogram (red solid line); mean value function (black dotted line); mean value plus/minus standard deviation functions (black dashed lines); envelope of the maximum and minimum values of all samples (shaded area). (For interpretation of the references to colour in this figure legend, the reader is referred to the Web version of this article.)

$$\psi_j(t) = \int_{t_{j-1}}^{t} \left[a(t_{j-1}) + \overline{a}_j(\tau) \right]^2 \mathrm{d}\tau\,, \quad t_{j-1} \le t < t_j; \tag{16}$$

where the function $\overline{a}_j(t)$ is here assumed as a polynomial of p-th order:

$$\begin{cases} \overline{a}_j(t) = \displaystyle\sum_{i=1}^{p} \alpha_i \ \left(t - t_{j-1}\right)^i, & t_{j-1} \le t < t_j; \\ \overline{a}_j(t) = 0, \quad t < t_{j-1}, & t \ge t_j. \end{cases} \tag{17}$$

The polynomial coefficients α_i can be evaluated by least-square fitting $\psi_j(t)$ to the accelerogram cumulative energy $E_{\ddot{U}_g}(t)$. That is, in the j-th time interval $[t_{j-1}, t_j)$, the following optimization problems have to be solved:

$$\begin{cases} \text{find } \alpha_1,\ \alpha_2, \cdots \alpha_p; \\ \text{minimising} \quad \displaystyle\int_{t_{j-1}}^{t_j - \Delta t} \left[E_{\ddot{U}_g}(t) - \psi_j(t) \right]^2 dt; \quad j = 1, 2, \cdots, n_a - 1 \\ \text{such that } \ \overline{a}_j(t) \ge 0, \quad \overline{a}_j(t) = \displaystyle\sum_{i=1}^{p} \alpha_i \ \left(t - t_{j-1}\right)^i, \quad t_{j-1} \le t < t_j; \end{cases} \tag{18}$$

being Δt the sampling interval of the target accelerogram. Note that the upper limit of the integral, in the optimization problem, avoids the overlap between the values of the cumulative energy function at the extremes of chosen time intervals. This guarantees the continuity of modulating functions too.

In the last $(n_a - \text{th})$ time interval with $t \in [t_{n_a - 1}, \quad t_{n_a} \equiv T_D]$, the *modulating function* is approximated by an exponential decaying function whose coefficients are evaluated by imposing the continuity with the

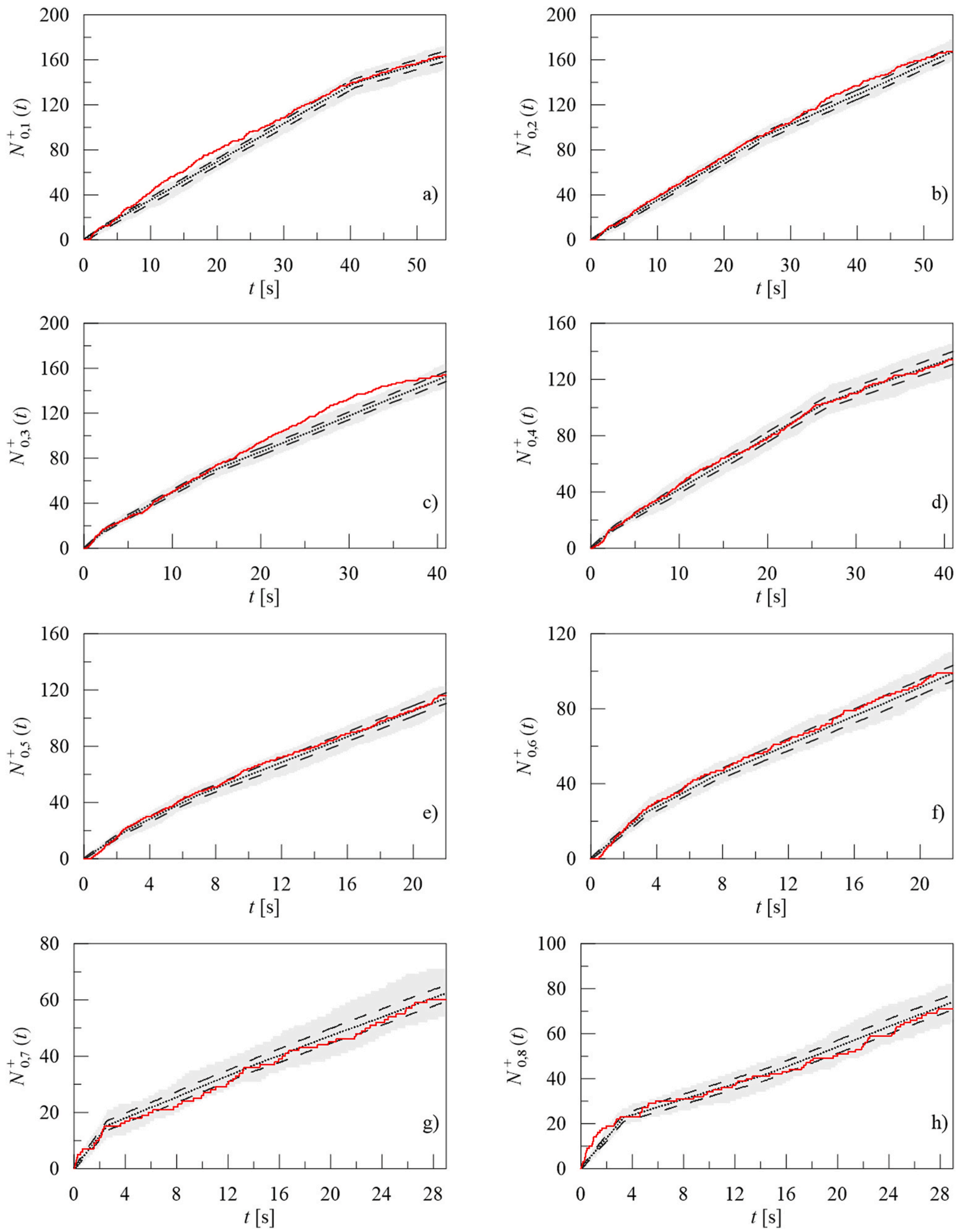

Fig. 6. Comparison among the zero-level up-crossings of the selected accelerograms with statistics of the artificial ones: a) Taft Lincoln School-21; b) Taft Lincoln School-111; c) Kakogawa-0; d) Kakogawa-90; e) Forgaria Cornino-0; f) Forgaria Cornino-270; g) Yarimca-60; h) Yarimca-150. Target accelerogram (red solid line); mean value function (black dotted line); mean value plus/minus standard deviation functions (black dashed lines); envelope of the maximum and minimum values of all samples (shaded area). (For interpretation of the references to colour in this figure legend, the reader is referred to the Web version of this article.)

Table 5
Mean values μ_{I_0}, $\mu_{N_0^+}$, standard deviations σ_{I_0}, $\sigma_{N_0^+}$, and coefficients of variation σ_{I_0}/μ_{I_0}, $\sigma_{N_0^+}/\mu_{N_0^+}$, of *total intensity* I_0, and of the total number of *zero-level up-crossing* N_0^+, for the eight analysed accelerograms.

n°	μ_{I_0} [m^2/s^3]	σ_{I_0} [m^2/s^3]	σ_{I_0}/μ_{I_0}	$\mu_{N_0^+}$	$\sigma_{N_0^+}$	$\sigma_{N_0^+}/\mu_{N_0^+}$
1	3.48	0.32	0.093	163.34	4.65	0.028
2	3.80	0.36	0.095	167.17	4.59	0.027
3	6.25	0.64	0.102	152.62	4.44	0.029
4	10.80	1.18	0.109	135.26	4.58	0.033
5	1.80	0.32	0.178	114.16	3.75	0.032
6	2.29	0.48	0.210	98.98	4.06	0.041
7	8.04	1.28	0.159	62.32	2.92	0.046
8	8.00	1.47	0.184	74.02	3.37	0.045

previous one and its decaying down to the absolute value, $\left|\ddot{U}_g(T_D)\right|$, at the end of the target accelerogram:

$$a(t) = a(t_{n_a-1})\exp\left[\frac{t-t_{n_a-1}}{T_D-t_{n_a-1}}\ln\left(\frac{\left|\ddot{U}_g(T_D)\right|}{a(t_{n_a-1})}\right)\right], \quad t_{n_a-1}\le t\le T_D. \tag{19}$$

Finally, once the functions $\overline{a}_j(t)$ are evaluated, the *modulating function* in the time interval $[0, T_D]$ can be written as:

$$\begin{aligned} a(t) &= \sum_{j=1}^{n_a-1}\overline{a}_j(t)\mathbb{W}(t_{j-1},t_j) \\ &+ a(t_{n_a-1})\exp\left[\frac{t-t_{n_a-1}}{T_D-t_{n_a-1}}\ln\left(\frac{\left|\ddot{U}_g(T_D)\right|}{a(t_{n_a-1})}\right)\right]\mathbb{W}(t_{n_a-1},T_D). \end{aligned} \tag{20}$$

It should be emphasised that for the estimation of the *modulating* *function*, in each generic time interval, only the evaluation of the energy of the target accelerogram in the same time-interval is required.

Notice that in the proposed procedure it could be also assumed $n_a \neq n$, n being the number of contiguous time intervals in which the *EPSD* function (12) of the stochastic process $F_0(t)$ is subdivided. Obviously, the assumption $n_a = n$ simplifies the procedure from a computational point of view.

4.2. Estimation of PSD function parameters

Since analysing the expected cumulative energy function of the fully non-stationary stochastic process $F_0(t)$, it is possible only to estimate the amplitude variation of the target accelerogram $\ddot{U}_g(t)$, another criterion to estimate the variation of the frequency content of $F_0(t)$ must be established, such that $\ddot{U}_g(t)$ may be considered as one of its samples. Once the time interval $0 \div T_D$ is divided in n contiguous time intervals, this purpose is here achieved by capturing in the generic k-th time interval a group of seismic waves possessing the specific frequency distribution of the target accelerogram in the same time interval. To do this the spectral parameters, Ω_k, ρ_k, $\omega_{H,k}$ and $\omega_{L,k}$, appearing in Eq. (8), of the one-sided *PSD* function $G_{X_k}(\omega)$ of the stationary sub-process $X_k(t)$ must be appropriately estimated.

It is well known that the frequency content of a recorded accelerogram $\ddot{U}_g(t)$ can be related to the frequency of occurrences of certain events. The most useful are: a) occurrences of both positive and negative maxima, here simply called *peaks*; b) occurrences of crossings of the time-axis with positive slope, commonly called *zero-level up-crossings*. For theoretical narrow-band zero-mean stationary stochastic process, the *zero-level up-crossings* frequency and *peaks* frequency are exactly the same and are coincident with the *mean frequency* of the process. For wider bandwidths, more than one peak occurs between two *zero-level up-crossings*. It follows that the ratio of the *zero-level up-crossings* frequency to the *peak* frequency, the so-called *irregularity factor* [64], gives a measure of the bandwidth of the process, i.e. how much the examined stochastic process differs from the narrow band one. To account for the irregularity of zero-mean stationary stochastic processes, Cartwright and Longuet-Higgins [65] introduced the *bandwidth parameter*, which can be evaluated as [66,67]:

$$\varepsilon = \sqrt{1 - \left(\frac{N_0^+}{P_0}\right)^2} \tag{21}$$

where N_0^+ and P_0 are the total number of *zero-level up-crossings* and the total number of *peaks* of target accelerogram. It follows that, having evaluated the *mean circular frequency*, $2\,\pi\,N_0^+/T_D$, a measure of the dispersion width of the *energy spectrum* of the target accelerogram $\ddot{U}_g(t)$ can be approximately evaluated by the following spectral parameter:

$$\delta = \frac{2\,\pi\,N_0^+}{T_D}\sqrt{1 - \left(\frac{N_0^+}{P_0}\right)^2} \tag{22}$$

In this paper, to capture the frequency content of the target accelerogram in the n contiguous time intervals in which T_D is divided, the number of *peaks*, P_k, and the number of *zero-level up-crossings*, $N_{0,k}^+$, in all time intervals, $[t_{k-1}, t_k)$, are evaluated. Since in the k-th time interval the stochastic process is assumed uniformly modulated, with *EPSD* function $a(t)\ G_{X_k}(\omega)$, the *zero-level up-crossing* frequency of target accelerogram, $N_{0,k}^+/\Delta T_k$, is very close to the *mean frequency* of the process and it can be reasonably assumed equal to the predominant circular frequency, Ω_k, of the k-th stationary sub-process. That is, the following relationship is written:

$$\Omega_k \cong \frac{2\,\pi\,N_{0,k}^+}{\Delta T_k} \tag{23}$$

In order to evaluate the circular frequency bandwidth parameter, ρ_k, of the unimodal one-sided *PSD* function $G_k^{(CP)}(\omega)$, given in Eq. (9), it needs to evaluate the convergent part of the second $\tilde{\lambda}_{1,X_k}^{(CP)}$ and third $\tilde{\lambda}_{2,X_k}^{(CP)}$ spectral moments as [see e.g. 68]:

$$\tilde{\lambda}_{1,X_k}^{(CP)} = \frac{\Omega_k^2 + \rho_k^2}{\Omega_k}\left[1 + \frac{\Omega_k^2 - \rho_k^2}{\pi(\Omega_k^2 + \rho_k^2)}\right]\arctan\left(\frac{\Omega_k}{\rho_k}\right); \tilde{\lambda}_{2,X_k}^{(CP)} = \Omega_k^2 - \rho_k^2\ ; \tag{24}$$

Relating, for every time interval $[t_{k-1}, t_k)$, the spectral parameter given in Eq. (22) to the radius of gyration, with respect to the centre of gravity, of the unimodal one-sided *PSD* function $G_k^{(CP)}(\omega)$, the following relationship can be written:

$$\delta_{X_k}^{(CP)} = \sqrt{\tilde{\lambda}_{2,X_k}^{(CP)} - \left(\lambda_{1,X_k}^{(CP)}\right)^2} \cong \frac{2\,\pi\,N_{0,k}^+}{\Delta T_k}\sqrt{1 - \left(\frac{N_{0,k}^+}{P_k}\right)^2} \tag{25}$$

After some algebra, it can be proved that the frequency bandwidth ρ_k of the function $G_k^{(CP)}(\omega)$ can be approximated as:

$$\rho_k \simeq \frac{\pi\,N_{0,k}^+}{2\,\Delta T_k}\left[\pi\ - 2\frac{N_{0,k}^+}{P_k}\right] \tag{26}$$

To complete the characterization of the one-sided *PSD* function $G_{X_k}(\omega)$, given in Eq. (8), the circular frequency control of two Butterworth filters $\omega_{H,k}$ and $\omega_{L,k}$ in all time intervals $[t_{k-1}, t_k)$, have to be estimated. In particular, the k-th high pass filter was introduced only to avoid very low frequency distortion of the *PSD* function $G_k^{(CP)}(\omega)$. On the contrary the k-th low pass filter was introduced for both to ensure the convergence of spectral moments until fourth order of the one-sided *PSD* function $G_{X_k}(\omega)$, and to reduce the gap between the number of *zero-level up-crossings* $N_{0,k}^+$ of target accelerogram and the expected number of *zero-level up-crossings* of the *fully non-stationary* process $F_0(t)$.

5. Numerical examples

In the previous sections the *fully-non stationary* zero-mean Gaussian process $F_0(t)$, was defined as the sum of zero-mean Gaussian *uniformly modulated* processes, defined in contiguous time intervals (see Eq. (12)). Then, a method for generating samples of a *fully non-stationary* zero-mean Gaussian process, in such a way that a given target accelerogram $\ddot{U}_g(t)$ can be considered as one of its own samples, was proposed.

In this section, in order to verify the accuracy of the proposed method, some statistics of a set of *fully non-stationary* Gaussian zero-mean artificial accelerograms having on average the cumulative energy functions and *zero-level up-crossings* of the target ones, are evaluated. The temporal variation of the amplitude is obtained through an appropriate estimate of the *modulating function* $a(t)$, while the variation in the frequency content of the generated samples is obtained by appropriately estimating the *PSD* functions of stationary sub-processes having unit variances. Since the sub-processes have unit variances, the *modulating function* and the main parameters characterizing the *PSD* functions, in the various time intervals, can be estimated separately.

The proposed procedure is applied to both the horizontal components of four seismic acceleration records, namely: Kern County (California, USA) 1952, Kobe (Japan) 1995, Friuli (Italy) 1976, Kocaeli (Turkey) 1999, downloaded from PEER database [69].

Table 1 lists the main characteristics of the analysed accelerograms: event name, station name and event date, moment magnitude M_w, site-source distance R_{JB} [70], peak ground acceleration a_{max} (i.e. the largest absolute value of the target accelerogram), average value of propagation velocity of S waves in the upper 30 m of the soil profile at the recording station v_{s30}, time duration of the analysed accelerogram T_D, significant strong motion duration *SMD* (i.e. interval of time elapsed between the 5% and 95% of the I_0), *total intensity* I_0, *Arias intensity* I_A [71], total number of *zero-level up-crossings* N_0^+ and total number of *peaks* P_0.

5.1.1. Estimation of the modulating function parameters of the analysed accelerograms

To evaluate the *modulating function* $a(t)$ of the uniformly modulated sub-processes, the time duration of the analysed accelerogram $0 \div T_D$, has to be divided in n_a time intervals. Two strategies can be adopted to obtain a good match between the expected cumulative energy function of artificial and target accelerograms: i) subdivide the target accelerogram in several time intervals (e.g. Der Kiureghian and Crempien [48] suggested at most nine frequency bands); ii) subdivide the time duration in only three time intervals $n_a = 3$, also optimizing the choice of instants of passage from one time interval to adjacent ones.

The second strategy is here adopted. Moreover, according to the models by Amin and Ang [21] and by Jennings et al. [23], the *modulating function* in the first time interval, $0 \le t < t_1$, is here assumed parabolically increasing from zero; while in the third time interval, $t_2 \le t \le T_D$, it is assumed exponentially decreasing, consistently with Eq. (20). In the second time interval, $t_1 \le t < t_2$, the assumption of constant *modulating function*, as proposed by Amin and Ang [21] and by Jennings et al. [23], leads to very unsatisfactory results for both energy and frequency content of the *fully non-stationary* process $F_0(t)$. Therefore, in the proposed approach, a polynomial of p-th order to model the *modulating function* in the second interval is adopted. It has been also observed that the choice of time instants t_1 and t_2 strongly influences both the energy and frequency content of the process $F_0(t)$. Hence, the proposed method requires an optimal choice of time instants t_1 and t_2, as well as of the order p of the polynomial *modulating function*. As a measure of the accuracy, the *root-mean-square* (*rms*) difference D_p, between the estimated *modulating function*, given in Eq. (20), and target accelerogram absolute values is defined as follows:

$$D_p = \sqrt{\frac{\Delta t}{T_D} \sum_{j=0}^{T_D/\Delta t} \left[a(j\,\Delta t) \; - \left| \ddot{U}_g(j\Delta t) \right| \right]^2} \tag{27}$$

where Δt is the sampling interval of the target accelerogram and the subscript p denotes the order of the polynomial considered in the second time interval.

Specifically, for the estimation of the *modulating function* the following steps are required:

a) in the first time interval, the *modulating function* $a(t)$, is assumed as a polynomial of second order; then the optimization problem described with reference to Eq. (18) for five values of $t_1 = t_{1\%}, t_{2\%}, \cdots, t_{5\%}$ ($t_{k\%}$ time instant in which the cumulative energy function of the accelerogram assumes the k% of its *total intensity*: $E_{\ddot{U}_g(t_{k\%}) \equiv k\,\% \times I_0}$) is solved;
b) in the second time interval it is assumed that the *modulating function* is a polynomial, the order of which, p, varies from one to ten; furthermore, different values of both time instant of passage from the first to the second interval, $t_1 = t_{1\%},\ t_{2\%}, \cdots, t_{5\%}$, and from the second to the third interval, $t_2 = t_{90\%},\ t_{91\%},\ \cdots,\ t_{99\%}$ are chosen;
c) in the third time interval $[t_2,\ T_D]$, according to Eq. (20), an exponential decay form for the *modulating function* is assumed; its initial value, $a(t_2)$ depends on the various combinations adopted for the *modulating function* in the second time interval.

Finally, among the various *modulating functions* obtained by applying the previously described procedure (varying the instants t_1 and t_2), the one characterised by the lowest *rms* difference D_p, is selected.

The parameters which characterise the selected *modulating functions* $a(t)$ are listed in Table 2, for all the selected accelerograms, together with the values of the time instants, t_1 and t_2, corresponding to the passage from one interval to another, the corresponding percentages of *total intensity*, k_1% and k_2%, the order p of the polynomial in the second time interval, the *rms* difference D_p, and the absolute value $\left|\ddot{U}_g(T_D)\right|$ at the end of the target accelerogram.

For the first two time intervals, the polynomial coefficients α_i, obtained through the optimization procedure, are listed in Table 3.

In Fig. 1, for the eight analysed accelerograms, the absolute value of each accelerogram together with the four *modulating functions* having the smaller *rms* difference D_p are plotted. This figure shows that small *rms* differences D_p can be obtained with different choices of the polynomial order and that often the highest order of the polynomial does not provide the smallest D_p. Furthermore, choosing the same polynomial order for all target accelerograms could give in many cases inaccurate results. For coherence in the following the polynomial order which gives the lowest D_p is adopted.

Finally, Fig. 2 shows that the moduli of Fourier transforms, $|\mathscr{F}[\bullet]|$, of the eight modulating functions of Fig. 1 are mainly concentrated in the region of zero frequency. This is in accord with Priestley's definition of a slowly varying function of time [46].

5.1.2. Estimation of the sub-processes PSD function parameters

The characterization of the *fully-non stationary* zero-mean Gaussian process $F_0(t)$ must be completed by estimating the parameters of the one-sided *PSD* function $G_{X_k}(\omega)$ of the stationary sub-process $X_k(t)$, appearing in Eq. (8). To do this, for the three time intervals of each of the eight analysed accelerograms $\ddot{U}_{g,\ell}(t)$, the predominant circular frequency Ω_k, and the bandwidth frequency parameters ρ_k, have to be evaluated. According to Eqs. (23) and (26), the evaluation of these parameters requires the counting of the number of *zero-level up-crossings* $N^+_{0,k}$, and the number of *peaks* P_k in the time intervals ΔT_k, of each accelerogram. The parameters useful to the characterization of the one-sided *PSD* function $G_{X_k}(\omega)$ are reported in Table 4. Finally, through several numerical tests it was verified that the control frequencies of two Butterworth filters $\omega_{H,k}$ and $\omega_{L,k}$ can be assumed equal to $\omega_{H,k} = 0.1\ \ \Omega_k$ and $\omega_{L,k} = \Omega_k + 0.8\rho_k$, respectively.

In Fig. 3, for the eight analysed accelerograms $\ddot{U}_{g,\ell}(t)$, the one-sided *PSD* functions $G_{X_k,\ell}(\omega)$ of the stationary sub-processes $X_{k,\ell}(t)$ are depicted. Curves in Fig. 3 represent the variation of the three *PSD* functions in the three contiguous time intervals, pointing out the time variation of the frequency content of target accelerograms. Analysing the results in Fig. 3, and the predominant circular frequencies listed in Table 4, it is apparent that the predominant frequencies Ω_k usually decrease with increasing time. However, in some cases, this condition is not completely satisfied.

5.1.3. Generation of artificial accelerograms

Once the parameters characterizing the *fully-non stationary* zero-mean Gaussian process, $F_0(t)$, defined in Eq. (7), are estimated, it is easy to generate its samples in such a way that the selected target accelerogram can be considered as one of its own samples. Indeed, according to the first of Eqs.(6), the i-th sample of the real part of the $F_0(t)$, containing in its set the target accelerogram $\ddot{U}_g(t)$, can be evaluated as:

$$\overline{F}_0^{(i)}(t) = a(t)\sqrt{2\Delta\omega} \times \left[\sum_{k=1}^{n} \sum_{r=1}^{m_N} \mathbb{W}(t_{k-1}, t_k) \sin\left(r\,\Delta\omega\,t + \theta_r^{(i)} \right) \sqrt{G_{X_k}(r\,\Delta\omega)} \right] \tag{28}$$

assuming a frequency increment $\Delta\omega = \omega_N / m_N = 0.1$, an upper cut-off circular frequency $\omega_N = 100$ rad/s, $m_N = 1000$ and $\Delta t = \pi/(4\omega_N)$. Note that the random phase angles, $\theta_r^{(i)}$, uniformly distributed over the interval $[0 - 2\pi)$, must be the same for all segments of the i-th sample.

Using this approach, a set of one hundred samples is evaluated for each of the selected accelerogram. In Fig. 4 the time-history of the eight analysed records, numbered in Table 1, is compared with one sample of the corresponding stochastic process (28) and a good similarity of the sample to the target accelerogram can be observed.

A more complete comparison can be performed by evaluating for the eight analysed accelerograms the cumulative energy functions $E_{\ddot{U}_{g,\ell}(t)}$ and cumulative *zero-level up-crossing* functions $N^{+}_{0,\ell}(t)$, which count the number of *zero-level up-crossing* until the time *t*. These two functions are compared, for each of the analysed accelerogram, with the corresponding mean value functions obtained by calculating the average of the results of the sets of artificial accelerogram samples.

In particular, in Fig. 5 the cumulative energy functions of the eight analysed target accelerograms are compared to those obtained as the mean value of the hundred samples. In Fig. 5 the cumulative energy function confidence intervals, evaluated as the mean values plus/minus the corresponding standard deviation, are also plotted. In Fig. 6 the cumulative *zero-level up-crossing* functions of target accelerograms are compared with the mean value functions of the one hundred samples and the cumulative *zero-level up-crossing* function confidence intervals. In Figs. 5 and 6, the shaded areas represent the envelope of the maximum and minimum values of the cumulative energy function and cumulative *zero-level up-crossing* of the 100 generated samples, respectively.

Figs. 5 and 6 evidence the accuracy of the proposed procedure. Note that the choice of the simple decreasing exponential function in the third time interval is paid for with a small difference in terms of *zero-level up-crossings* in the last time interval.

Note that although the generated accelerograms are samples of a zero-mean Gaussian process, the corresponding cumulative energy function and the cumulative *zero-level up-crossing* function are not zero-mean Gaussian processes. To evidence this, the mean values μ_{I_0}, $\mu_{N_0^+}$, the standard deviations σ_{I_0}, $\sigma_{N_0^+}$, and the coefficients of variation σ_{I_0}/μ_{I_0}, $\sigma_{N_0^+}/\mu_{N_0^+}$ of *total intensity* I_0 and of the total number of *zero-level up-crossing* N_0^+ are reported in Table 5, for the eight analysed accelerograms.

6. Conclusions

For several practical applications concerning non-linear dynamic analyses of both structural and geotechnical aspects, the need of generating artificial accelerograms having frequency and energy content and distribution of number of cycles consistent with actual acceleration records, is manifest.

In this vein, a method for generating samples of a *fully non-stationary* zero-mean Gaussian process, in such a way that the chosen target accelerogram can be considered as one of its own samples, is presented in the paper. In the proposed method, once the target accelerogram is subdivided in some contiguous time intervals, the computation of the cumulative energy and the cumulative counts of *zero-level up-crossings* as well as negative and positive maxima (the so-called *peaks*) is required.

The evolutionary *power spectral density* (*PSD*) function of the proposed fully non-stationary process model is evaluated as the sum of uniformly modulated processes. These are defined in each time interval, as the product of deterministic modulating functions per stationary zero-mean Gaussian sub-processes, whose unimodal *PSD* functions are filtered by high pass and low pass Butterworth filters. In each time interval the parameters of *modulating functions* are estimated by least-square fitting the expected energy of the proposed model to the energy of the target accelerogram, while the parameters of *PSD* functions of stationary sub-processes are estimated once both occurrences of *peaks* and of *zero-level up-crossings* of the target accelerogram, in the various intervals, are counted. There is no need for sophisticated processing of the recorded motion such as Fourier transform.

In the numerical example, applications using as target accelerograms both horizontal acceleration components of four recorded seismic events are described in detail. A practical application of the proposed procedure to a set of four target horizontal acceleration time-histories is also presented and discussed in the paper.

In particular, according to various models proposed in the literature [21,23,47], the accelerograms are subdivided in three contiguous intervals in which appropriate unimodal *PSD* functions and polynomial forms of modulating functions have been chosen to obtain realistic seismic motion useful in the evaluation of the dynamic response of structural and geotechnical systems. The examples described in the paper demonstrate the effectiveness of the proposed parameter estimation method and the accuracy of the model in reproducing realizations with statistical characteristics similar to those of the target motion.

As a final remark it is important to stress that, despite the proposed procedure was presented and described with reference to a single target accelerogram, it can be extended to account for the variability of the expected ground motion considering the uncertainties inherent to the values of the seismic parameters assumed as targets in the generation procedure.

CRediT authorship contribution statement

G. Muscolino: Conceptualization, Methodology, Supervision, Formal analysis, Writing - review & editing. **F. Genovese:** Conceptualization, Methodology, Formal analysis, Data curation, Software, Supervision, Writing - review & editing. **G. Biondi:** Conceptualization, Writing - review & editing. **E. Cascone:** Conceptualization, Writing - review & editing.

Declaration of competing interest

The authors declare that they have no known competing financial interests or personal relationships that could have appeared to influence the work reported in this paper.

Acknowledgements

This work is part of the research activities carried out in the framework of the research project of major national interest, PRIN n. 2017YPMBWJ, on “Risk assessment of Earth Dams and River Embankments to Earthquakes and Floods (REDREEF)” funded by the Italian Ministry of Education University and Research (MIUR).

Appendix A. Supplementary data

Supplementary data to this article can be found online at https://doi.org/10.1016/j.soildyn.2020.106467.

References

[1] Villaverde R. Fundamental concepts of earthquake engineering. Boca Raton, Florida, USA: CRC Press; 2009.
[2] Barone G, Lo Iacono F, Navarra G, Palmeri A. Closed-form stochastic response of linear building structures to spectrum consistent seismic excitations. Soil Dynamics and Earthquake Engineering 2019;125:e102749. https://doi.org/10.1016/j.soildyn.2019.105724.
[3] Bommer JJ, Acevedo AB. The use of real earthquake accelerograms as input to dynamic analysis. Journal of Earthquake Engineering 2004;8(1):43–91. https://doi.org/10.1142/S1363246904001596.
[4] Iervolino I, Galasso C, Cosenza E. REXEL: computer aided record selection for code-based seismic structural analysis. Bulletin of Earthquake Engineering 2010;8: 339–62. https://doi.org/10.1007/s10518-009-9146-1.
[5] Katsanos EI, Sextos AG, Manolis GD. Selection of earthquake ground motion records: a state-of-the-art review from a structural engineering perspective. Soil Dynam Earthq Eng 2010;30(4):157–69. https://doi.org/10.1016/j.soildyn.2009.10.005.
[6] Pagliaroli A, Lanzo G. Selection of real accelerograms for the seismic response analysis of the historical town of Nicastro (Southern Italy) during the March 1638 Calabria earthquake. Eng Struct 2008;30:2211–22.
[7] Genovese F, Aliberti D, Biondi G, Cascone E. A procedure for the selection of input ground motion for 1D seismic response analysis. In: Proceedings of 7ICEGE; 2019. p. 2591–8. Rome, Italy.

[8] Genovese F, Aliberti D, Biondi G, Cascone E. Geotechnical aspects affecting the selection of input motion for seismic site response analysis. Eccomas Proceedia Compdyn 2019:151–61. https://doi.org/10.7712/120119.6909.19616.
[9] Lanzo G, Pagliaroli A, Scasserra G. Selection of ground motion time histories for the nonlinear analysis of earth dams. XVI ECSMGE 2015, geotechnical engineering for infrastructure and development, 2031–2036.
[10] Cascone E, Biondi G, Aliberti D, Rampello S. Effect of vertical input motion and excess pore pressures on the seismic performance of a zoned dam. Soil Dynamics and Earthquake Engineering; 2020. Submitted for publication.
[11] Housner GW. Characteristics of strong-motion earthquakes. Bull Seismol Soc Am 1947;37:19–31.
[12] Bycroft GN. White noise representation of earthquakes. J Eng Mech (ASCE) 1960; 86:1–16.
[13] Kanai K. Semi-empirical formula for the seismic characteristics of the ground. Bull. Earthq. Res. Inst. 1957;35:309–25. University of Tokyo.
[14] Tajimi H. A statistical method of determining the maximum response of a building structure during an earthquake. In: Proc. 2nd WCEE, Tokyo, 2; 1960. p. 781–97.
[15] Clough RW, Penzien J. Dynamics of structures. New York: Mc Graw-Hill; 1975.
[16] Housner GW, Jennings PC. Generation of artificial earthquakes. J Eng Mech (ASCE) 1964;90:113–50.
[17] Faravelli L. Stochastic modeling of the seismic excitation for structural dynamics purposes. Probabilist Eng Mech 1988;3:189–95.
[18] Alderucci T, Muscolino G, Urso S. Stochastic analysis of linear structural systems under spectrum and site intensity compatible fully non-stationary artificial accelerograms. Soil Dynam Earthq Eng 2019;126:e105762. https://doi.org/10.1016/j.soildyn.2019.105762.
[19] Rezaeian S, Der Kiureghian A. A stochastic ground motion model with separable temporal and spectral nonstationarities. Earthq Eng Struct Dynam 2008;37:1565–84.
[20] Shinozuka M, Sato Y. Simulation of nonstationary random processes. J Eng Mech (ASCE) 1967;93:11–40. 1967.
[21] Amin M, Ang AH-S. Non-stationary stochastic models of earthquake motion. J Eng Mech (ASCE) 1968;94:559–83.
[22] Iyengar RN, Iyengar KT. Nonstationary random process for earthquake acceleration. Bull Seismol Soc Am 1969;59:1163–88.
[23] Jennings PC, Housner GW, Tsai NC. Simulated earthquake motions. Earthquake Engineering Research Laboratory, California Institute of Technology; 1968. Technical report.
[24] Hsu T-I, Bernard MC. A random process for earthquake simulation. Earthq Eng Struct Dynam 1978;6:347–62.
[25] Iwan WD, Hou ZK. Explicit solutions for the response of simple systems subjected to non-stationary random excitation. Struct Saf 1989;6:77–86.
[26] Stafford PJ, Sgobba S, Marano GC. An energy-based envelope function for the stochastic simulation of earthquake accelerograms. Soil Dynam Earthq Eng 2009; 29:1123–33.
[27] Marano GC. Non-stationary stochastic modulation function definition based on process energy release. Physica A 2019;517:280–9.
[28] Yeh CH, Wen YK. Modelling of nonstationary ground motion and analysis of inelastic structural response. Struct Saf 1990;8:281–98.
[29] Conte JP. Effects of earthquake frequency nonstationarity on inelastic structural response. In: Proc. 10th WCEE. Balkema, Rotterdam, The Netherlands, 7; 1992. p. 3645–51.
[30] Beck JL, Papadimitriou C. Moving resonance in nonlinear response to fully nonstationary stochastic ground motion. Probabilist Eng Mech 1993;8:157–67.
[31] Wang J, Fan L, Qian S, Zhou J. Simulations of non-stationary frequency content and its importance to seismic assessment of structures. Earthq Eng Struct Dynam 2002;31:993–1005.
[32] Der Kiureghian A. A coherency model for spatially varying ground motions. Earthq Eng Struct Dynam 1996;25:99–111.
[33] Guodong Z. Response analysis of the soil-structure inelastic interaction system under evolutionary random excitations. Ind Constr 2005;12.
[34] Wang ZH, Hu QX. Non-stationary stochastic seismic analysis of homogeneous earth dam. J. Disaster Prevent. Mitig. Eng. 2010;1.
[35] Bi KM, Hao H. Influence of irregular topography and random soil properties in coherency loss of spatial seismic ground motions. Earthq Eng Struct Dynam 2011; 40:1045–61.
[36] Wu YX, Gao YF, Zhang N, Li DY. Simulation of spatially varying ground motions in V-shaped symmetric canyons. J Earthq Eng 2016;20:992–1010.
[37] Spanos PD. Probabilistic earthquake energy spectra equations. J Eng Mech (ASCE) 1980;106:147–59.
[38] Spanos PD, Solomos GP. Markov approximation to transient vibration. J Eng Mech (ASCE) 1982;109:1134–50.
[39] Fan FG, Ahmadi G. Nonstationary Kanai-Tajimi models for El Centro 1940 and Mexico City 1985 earthquakes. Probabilist Eng Mech 1990;5:171–81.
[40] Rofooei FR, Mobarake A, Ahmadi G. Generation of artificial earthquake records with a nonstationary Kanai–Tajimi model. Eng Struct 2001;23:827–37.
[41] Lin YK. Nonstationary excitation and response in linear systems treated as sequences of random pulses. J Acoust Soc Am 1965;38:453–60.
[42] Liu SC. Synthesis of stochastic representations of ground motions. Bell Syst. Tech. J. 1970;49:521–41.
[43] Lin YK. On random pulse train and its evolutionary spectral representation. Probabilist Eng Mech 1986;1:219–23.
[44] Lin YK, Yong Y. Evolutionary Kanai-Tajimi earthquake models. J Eng Mech (ASCE) 1987;113:1119–37.
[45] Priestley MB. Evolutionary spectra and non-stationary random processes. J Roy Stat Soc B 1965;27:204–37.
[46] Priestley MB. Power spectral analysis of non-stationary random processes. J Sound Vib 1967;6:86–97.
[47] Saragoni GR, Hart GC. Simulation of earthquake ground motions. Earthq Eng Struct Dynam 1973;2:249–67.
[48] Der Kiureghian A, Crempien-Laborie JE. An evolution model for earthquake ground motion. Struct Saf 1989;6:235–46.
[49] Conte JP, Peng B-F. Fully nonstationary analytical earthquake ground-motion model. J Eng Mech (ASCE) 1997;123:15–24.
[50] Narasimhan SV, Pavanalatha S. Estimation of evolutionary spectrum based on short time Fourier transform and modified group delay. Signal Process 2004;84: 2139–52.
[51] Liang J, Chaudhuri SR, Shinozuka M. Simulation of nonstationary stochastic processes by spectral representation. J Eng Mech (ASCE) 2007;133:616–27.
[52] Spanos PD, Failla G. Evolutionary spectra estimation using wavelets. J Eng Mech (ASCE) 2004;130:952–60.
[53] Spanos PD, Tezcan J, Tratskas P. Stochastic processes evolutionary spectrum estimation via harmonic wavelets. Comput Methods Appl Mech Eng 2005;194: 1367–83.
[54] Wang D, Fao Z, Hao S, Zhao D. An evolutionary power spectrum model of fully nonstationary seismic ground motion. Soil Dynam Earthq Eng 2018;105:1–10.
[55] Huang TL, Lou ML, Chen HP, Wang NB. Hilbert-Huang transform and its application in the spectral representation of earthquake accelerograms. Soil Dynam Earthq Eng 2018;104:378–89.
[56] Garcia SR, Romo MP, Alcántara L. Analysis of non-linear and non-stationary seismic recordings of Mexico City. Soil Dynam Earthq Eng 2018;127:e105859. https://doi.org/10.1016/j.soildyn.2019.105859.
[57] Muscolino G, Alderucci T. Closed-form solutions for the evolutionary frequency response function of linear systems subjected to separable or non-separable non-stationary stochastic excitations. Probablistic Eng. Mech. 2015;40:75–89.
[58] Di Paola M. Transient spectral moments of linear systems. SM Arch 1985;10: 225–43.
[59] Di Paola M, Petrucci G. Spectral moments and pre-envelope covariances of nonseparable processes. J Appl Mech (ASME) 1990;57:218–24.
[60] Muscolino G. Nonstationary Pre-envelope covariances of nonclassically damped systems. J Sound Vib 1991;149:107–23.
[61] Michealov G, Sarkani S, Lutes LD. Spectral characteristics of nonstationary random processes-a critical review. Struct Saf 1999;21:223–44.
[62] Shinozuka M, Jan CM. Digital simulation of random process and its applications. J Sound Vib 1972;25:111–28.
[63] Chang FK, Franklin AG. PGA, RMSA, PSDF, duration, and MMI. In: Cakmak AS editor. Ground Motion and engineering seismology. Amsterdam: Elsevier Science Publishers B.V; 1987. p. 449–66.
[64] Lutes LD, Sarkani S. Random vibrations - analysis of structural and mechanical vibrations. Boston: Elsevier Inc.; 2004.
[65] Cartwright DE, Longuet-Higgins MS. The statistical distribution of the maxima of a random function. Proc Roy Soc Lond Math Phys Sci 1956;237:212–32.
[66] Wirshing PH, Paez TL, Keith O. Random vibrations: theory and practice. New York: Dover; 1995.
[67] Solnes J. Stochastic processes and random vibrations: theory and practice. John Wiley & Sons Inc; 1997.
[68] Di Paola M, Muscolino G. On the convergent parts of high order spectral moments of stationary structural responses. J Sound Vib 1986;110:233–45.
[69] Ancheta TD, Darragh RB, Stewart JP, Seyhan E, Silva WJ, Chiou BS-J, Wooddell KE, Graves RW, Kottke AR, Boore DM, Kishida T, Donahue JL. PEER NGA-West2 database. California: Pacific Earthquake Engineering Research Center/ 03; 2013.
[70] Joyner WB, Boore DM. Peak horizontal acceleration and velocity from strong motion records including records from the 1979 Imperial Valley, California, earthquake. Bull Seismol Soc Am 1981;71:2011–38.
[71] Arias A. A measure of earthquake intensity. In: Hansen RJ, editor. Seismic design for nuclear power plants. Cambridge: MIT Press; 1970. p. 438–83.